Chapter

Summary of Some Selected Characterization Methods of Geopolymers

Dattaguru Ananthapadmanaban

Abstract

All modern day materials have to be characterized in order to understand their properties. Simple techniques can be used for macrostructural and microstructural characterization. Many a time, however, advanced techniques may be required in order to understand structure property relationships in a better way. Advanced characterization techniques include scanning electron microscope (SEM), transmission electron microscope TEM, nuclear magnetic resonance (NMR), synchrotron, X-ray fluorescence microscopy and a few others. Geopolymers have advanced to the level of nanogeopolymers, and in order to understand the fundamental properties of nanogeopolymers, it becomes imperative to gain a fundamental understanding of characterization methods. SEM, TEM, NMR and synchrotrons have been briefly described, and advances in these characterization techniques have been emphasized. Microstructures of common geopolymers have been discussed with special emphasis on nanogeopolymers.

Keywords: SEM, TEM, X-rays, NMR, synchrotron

1. Introduction

Characterization studies are essential to gain practical knowledge about materials. They can also be used to correlate structure with properties. There is a host of characterization techniques used to identify materials. They include scanning electron microscopy, transmission electron microscopy, X-ray diffraction, TEM, XRD, X-ray fluorescence, NMR (nuclear magnetic resonance) and synchrotron techniques. However, no single technique can give a full analysis of the material being characterized. In practical research work, conclusions have to be drawn by using 2 or 3 characterization techniques. This chapter examines the use of various characterization techniques for researching geopolymers.

Aluminosilicate binder gel has an amorphous structure. Some years back, a study of amorphous structures was not possible since characterization techniques had not advanced to that extent. But, now it is possible to study amorphous structures, and hence characterization of geopolymers, which can occur in the amorphous state, is possible. Most of the literature in geopolymers concentrates on cements and substitutions/additions to cement. An additional advantage is the high compressive strength of geopolymers. Many geopolymers are manufactured using binders, and most of these binders exist in an amorphous state. These binders are

obtained by the reaction between an alkali source and a solid aluminosilicate powder. The aluminosilicate can be one among metakaolin, fly ash and/or blast-furnace slag. These geopolymers are increasingly being used as construction materials to replace Portland cement [1–3]. Geopolymers based on natural zeolite have also been studied and found to have good adhesion to concrete. These geopolymers have been characterized using XRD and SEM [4]. Fly ash has also been activated by alkali to form a geopolymer, but there are concerns regarding mechanical properties of this material [5]. Geopolymers based on phosphoric acid and illito-kaolinitic clay have been synthesized with reasonably good compression strength [6]. Hence, among all the geopolymers studied, kaolinite-based geopolymers seem to hold promise for the future, and this geopolymer has been used mainly for description of characterization.

Characterization methods have been classified into (a) microscopy (b) X-ray-based tomography and fluorescence (c) and other modern methods of characterization which include imaging, nuclear magnetic resonance, FTIR spectra and synchrotron. Each division of characterization has been described briefly before taking up case studies. Selective characterization techniques have been described with metakaolin as an example. Other geopolymers have also been characterized as and when required. During the description of selective characterization techniques, the use of characterization in metakaolin has been dealt with first, and then some more examples of characterization of other geopolymers have been studied as and when required.

2. Microscopy

Microscopy is commonly used in research and lab studies to throw light upon the detailed features of a material. Optical micrographs are generally used to study the metallurgical microstructures. But, in the case of geopolymers, we are concerned with the pore formation, distribution and other more intricate features. So either scanning electron microscope (SEM) or transmission electron microscope (TEM) is used in recent research. **Figure 1** summarizes the types of rays that are produced when an electron hits a sample target.

Electron beams strike the surface of the sample in all cases of electron microscopy. It would be worthwhile to have a short discussion of what happens when the electron beam strikes the surface. The **Figure 1** shown above gives a gist of the type of rays emitted after striking a sample. The backscattered electrons are used in SEM backscattered image. Unscattered electrons are used in TEM. Auger electrons are used in Auger spectroscopy, and emitted X-rays are used in EDS (electron dispersive spectra) and EPMA (electron probe microanalysis).

2.1 SEM imaging

Scanning electron microscopy has been widely used to study fractured surfaces. The images give an idea of whether the fracture is ductile or brittle. Sometimes, it is possible to have a mixed mode failure too (**Figure 2**).

2.2 TEM imaging

Figure 3 shown above gives in brief the differences between SEM and TEM. Here, the specimens have to be prepared to thin slices of less than 100 nm thickness. Again, similar to SEM, specimen preparation is of utmost importance. Vacuum has to be maintained in the TEM, and any flaw in the maintenance of

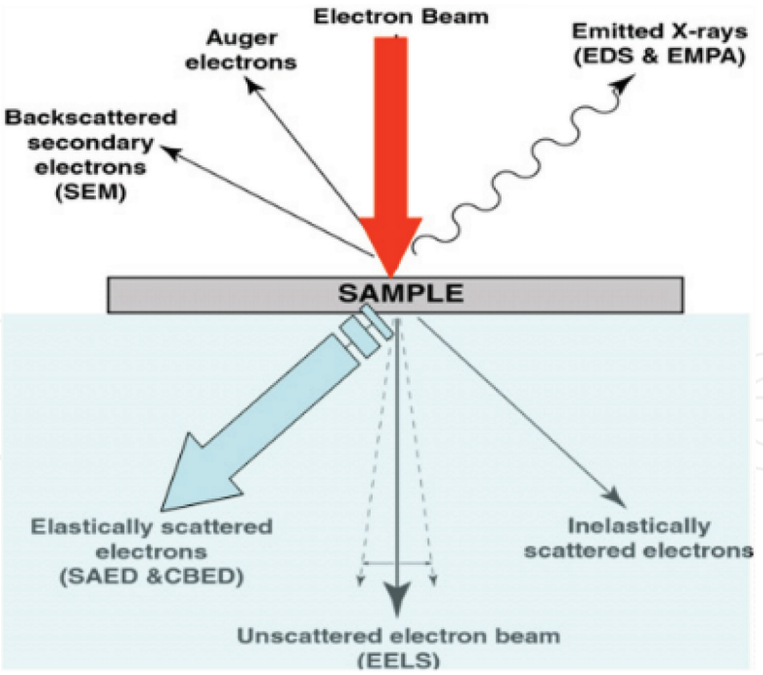

Figure 1.
Different types of reflected and transmitted rays.

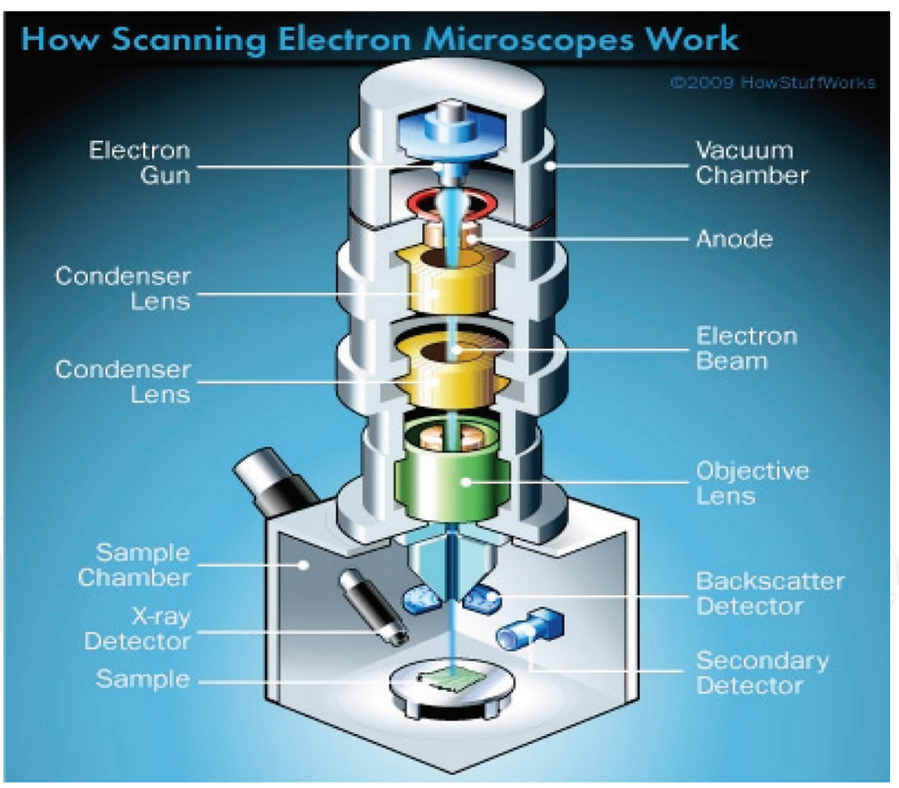

Figure 2.
Working principle of SEM—source [7].

vacuum will reflect in the performance of the TEM. Usually, dislocation density and second phase precipitation can be clearly seen in TEM images.

The electron gun is a source of electrons. The electrons are focused with the help of condenser lens and objective lens. There is a chamber to hold the workpiece. Care should be taken to prepare the workpiece very carefully and specialists are required for SEM sample preparation. The chamber consists of a backscatter detector and a secondary detector. So the SEM can be operated under two modes.

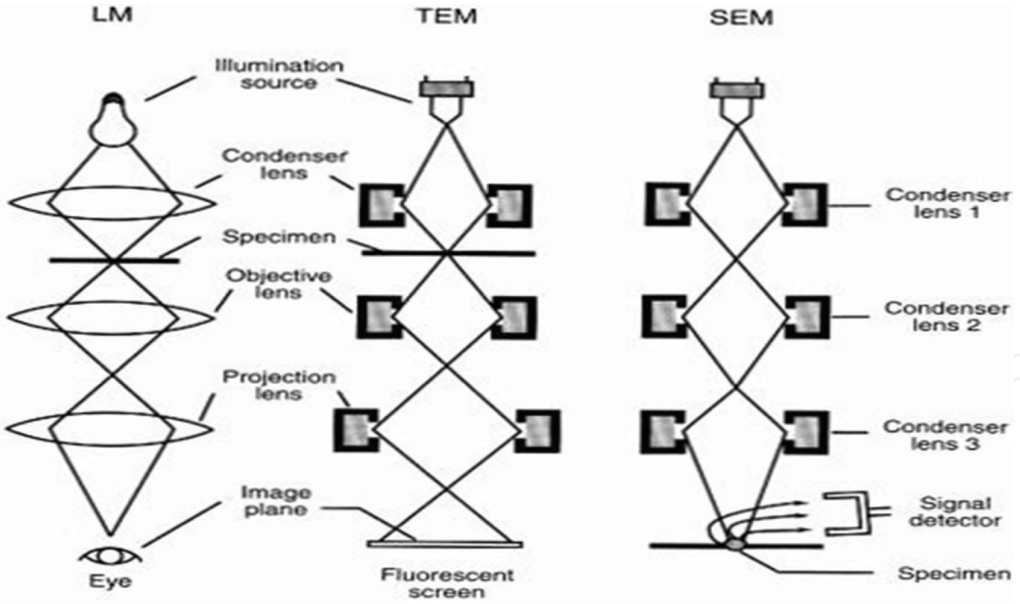

Figure 3.
Difference between light microscope, SEM and TEM.

Figure 4 depicts uniform distribution of metakaolin and possibly a ductile fracture. The SEM image above shows a wide variety of shapes of fly ash, tending towards a spherical shape. There seems to be agglomeration and there also seem to be some cracks. Cracks often lead to brittleness. This SEM micrograph of a fly ash geopolymer seems to indicate mixed mode of failure (**Figures 5** and **6**).

Again, this SEM shows an even wider distribution of particles and a very large particle size distribution too. It appears, from the cracks seen and the fragments in the SEM that in this case, there has been a brittle fracture. This possibility is supported by the fact that most concrete fails in a brittle fashion. Addition of geopolymer/substitution of various geopolymeric elements like fly ash could change the morphology and influence fracture to some extent.

Research in these areas is still in the nascent stage. However, it is worth mentioning here that considering the danger that Mother Earth is facing under the deluge of huge amounts of metallic and ceramic waste, it would be a very worthwhile task to look for alternatives to concrete or make some substitutions to concrete to make it more environmentally friendly. It is here that geopolymeric materials could help (**Figure 7**).

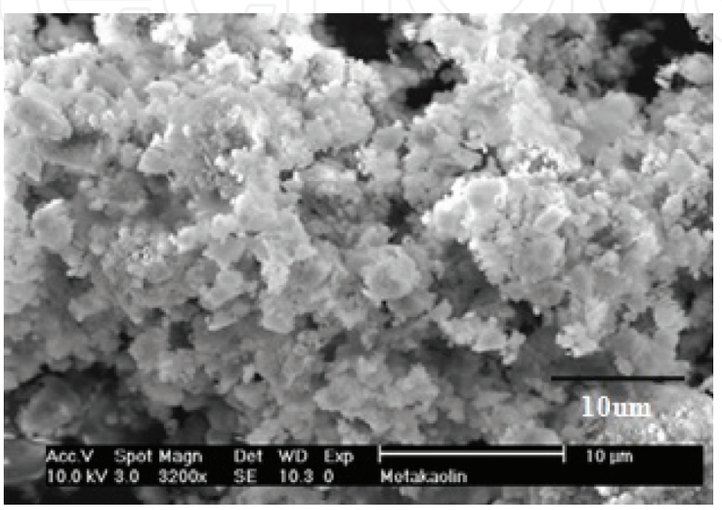

Figure 4.
SEM image of metakaolin; source—Wiki Image [8].

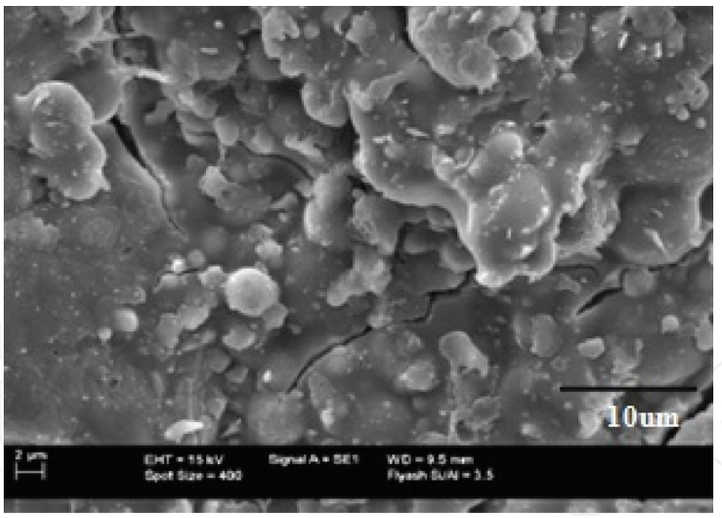

Figure 5.
SEM image of geopolymer fly ash after heating at 820 Celsius—courtesy of Temujin et al. [9].

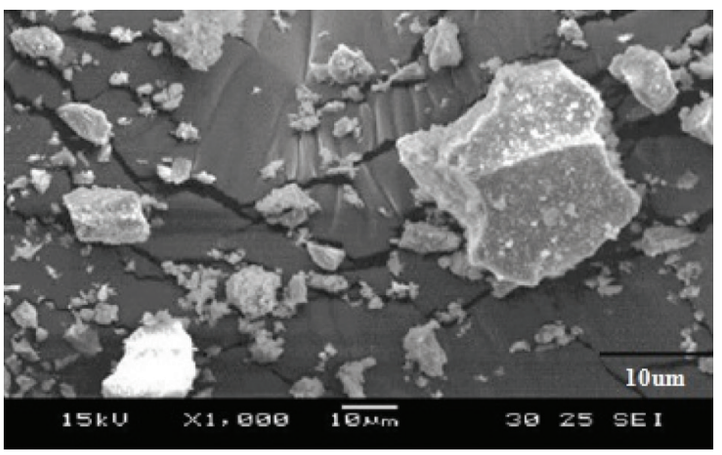

Figure 6.
SEM micrograph of fly ash geopolymer [10].

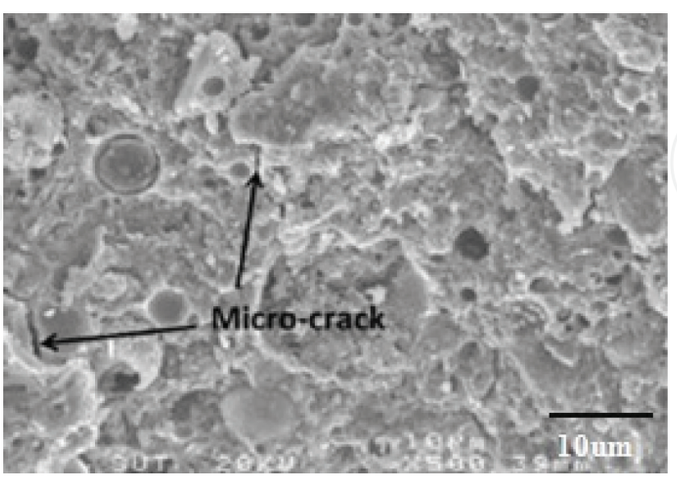

Figure 7.
SEM micrograph clay-based geopolymer brick cured at 85 Celsius for 24 hours [11].

Here, since the geopolymer is clay-based, the SEM shows a ductile type of fracture. Curing may be necessary to improve strength and bonding. Usage without curing may lead to lower tensile strength. Microcrack formations are seen in the SEM, but these are too small to be of any importance or create any immediate

danger of failing to the geopolymer. Another study of ground-granulated blast-furnace slag (GGBS)-amended fly ash was conducted by Sharma AK et al. This can be used as soil conservative. The SEM shown below shows a fairly ductile fracture. The interface condition is good and porosity is not seen. This indicates that there is good contact between soil particles and cementitious mix. C-S-H and calcium oxide formations have also been confirmed in this study. SEM evidence has shown that fly ash mixed with GGBS has the potential to improve the properties of expansive soil with a minimum requirement of chemical additives such as lime (**Figure 8**).

In **Figure 9**, clustering can be seen. The bright-field transmission electron micrograph of a slag-based geopolymer is shown in **Figure 9**. The figure shows the clustering of slag. This may have a deleterious effect on properties.

In **Figure 10(a)** Medri et al. [8] tested two metakaolins manufactured industrially by the company Imerys with two different kiln technologies. One called M1000 is calcined in a rotary kiln and characterized by rounded massive aggregates of lamellar particles. The second, called M1200S, calcined in a flash kiln, is made up of fine lamellar particles with lower agglomeration. **Figure 10(b)** reports that the geopolymer structure is characterized by gel (amorphous) phase, and also some crystalline phases are present as in most geopolymers.

TEM image shows agglomeration of slag, which can be seen with SEM also, but SEM can be used only for surface studies, whereas TEM can be used to find details of subsurface.

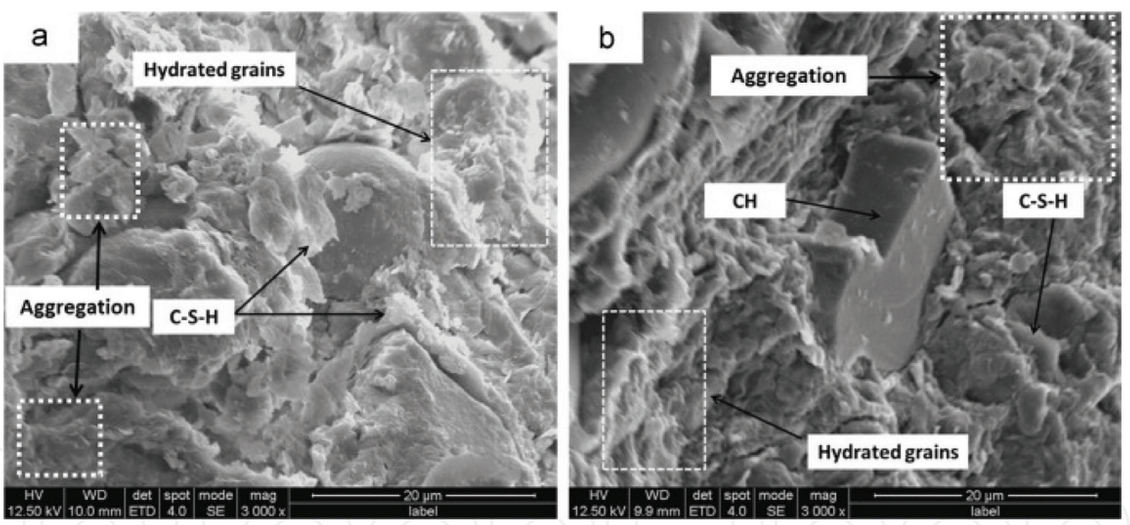

Figure 8.
C-S-H bonds and aggregation [10].

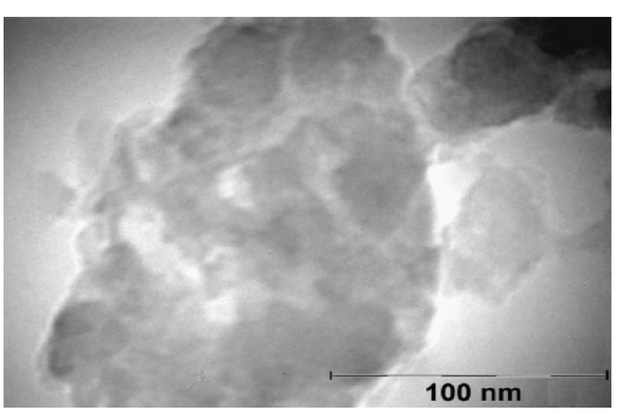

Figure 9.
Bright-field image of slag-based geopolymer.

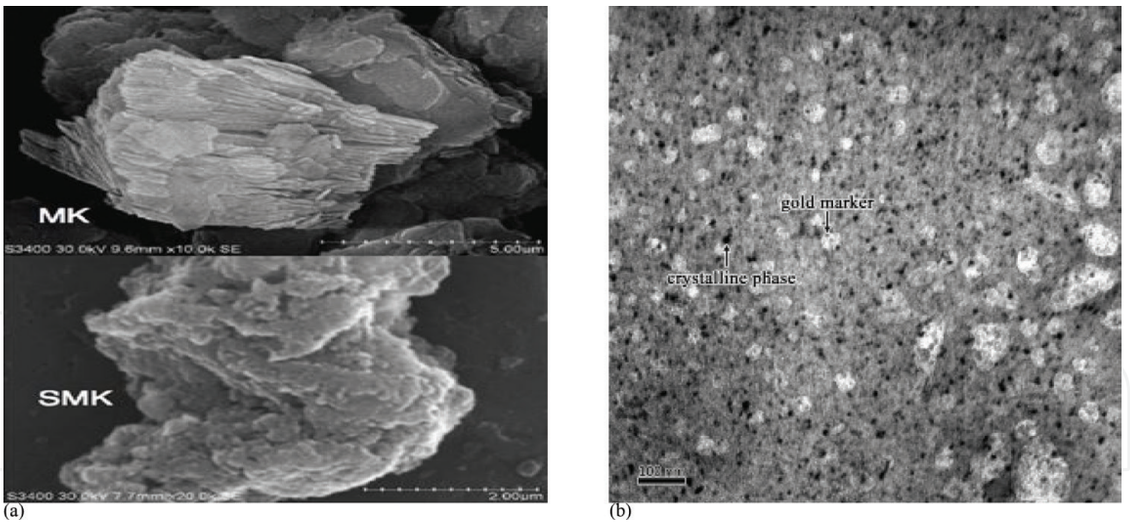

Figure 10.
(a) SEM images of natural and synthetic metakaolins (Cui et al.) [12] and (b) pore structure in coal ash-based geopolymer [13].

3. X-ray tomography and fluorescence microscopy

Many different cross-sectional views are created suing X-rays. These are then assembled to create a 3D image of the object. The size of the pixels which are created in this manner so created are in micrometers and hence the word, microtomography. It should be noted that the 3D model is a virtual model and is not in real time. These pixel sizes have also resulted in the terms high-resolution X-ray tomography, micro-computed tomography (micro-CT or μCT) and similar terms. In today's terminology, tomography automatically implies computer tomography.

Figure 11 illustrates the features of a slag-based geopolymer using the X-ray microtomograph. Furthermore, histogram, **Figure 11**, also depicts particle size distribution. In general, fly ash-based polymers have been studied by Das et al. and characterized by X-ray tomography [14].

The X-ray tomography shows the distribution of phases. Slag particles can be clearly seen as a white product. There also seem to be some cracks, which, if allowed to propagate, could lead to premature failure of the component in use (**Figure 12**).

According to The Royal Chemical Society, X-Ray Fluorescence is an imaging technique where a beam of X-rays is directed at the specimen-Rays are emitted

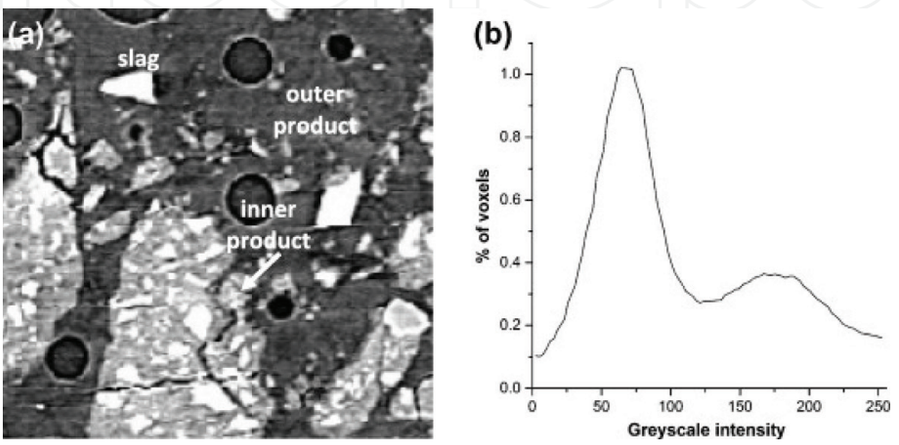

Figure 11.
X-ray microtomography scan of a sodium silicate-activated binder (80% slag/20% metakaolin, activat) (b) a histogram depicting volume of pixels of the volume of interest.

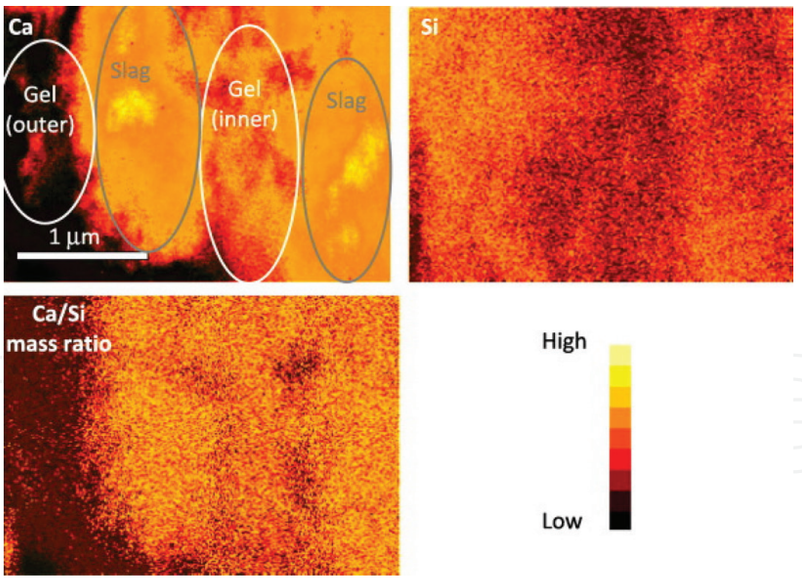

Figure 12.
X-ray fluorescence micrographs of a sodium metasilicate-activated binder (75% slag/25% metakaolin) [13].

due to transitions and the intensities of the X-rays emitted due to are detected as a function of wavelength and position. As these energies are element-specific, X-ray fluorescence microscopy can be used to determine spatially resolved elemental composition.

The X-Ray fluorescence image shown above shows different emitted colors for inner gel and for outer gel. As can be seen, the differences in Ca/Si ratio also can be mapped based upon the color.

4. Nuclear magnetic resonance (NMR) spectra

Nuclear magnetic resonance (**NMR**) is a physical phenomenon in which nuclei in a strong static magnetic field are perturbed by a weak oscillating magnetic field. This field is very close to the surface. It does not involve electromagnetic interactions or waves and respond by producing an electromagnetic signal with a frequency characteristic of the magnetic field at the nucleus. This process occurs near resonance. As we are aware, during resonance, two frequencies have to match, and the resultant frequency is far ahead in intensity compared to the two participating frequencies. When the oscillation frequency matches the intrinsic frequency of the nuclei, which depends on the strength of the static magnetic field, the chemical environment and the magnetic properties of the isotope involved; in practical applications with static magnetic fields up to ca. 20 tesla, the frequency is similar to VHF and UHF television broadcasts (60–1000 MHz). NMR results from specific magnetic properties of certain atomic nuclei. Nuclear magnetic resonance spectroscopy is widely used to determine the structure of organic molecules in solution and study molecular physics, crystals as well as noncrystalline materials. NMR is also routinely used in advanced medical imaging techniques, such as in magnetic resonance imaging (MRI).

Nuclear magnetic resonance spectra can be used to identify elemental groups. Each group has a characteristic shift in wavelength. The shifts for different geopolymers are shown in **Figure 14**.

Figure 13 depicts wavelength shift [15].

Figure 14 depicts the difference between amorphous and semi-crystalline geopolymers. Mathematical analysis has been done on these peaks, and Gaussian peak deconvolution has been used to characterize short range order in T-O-T bonds,

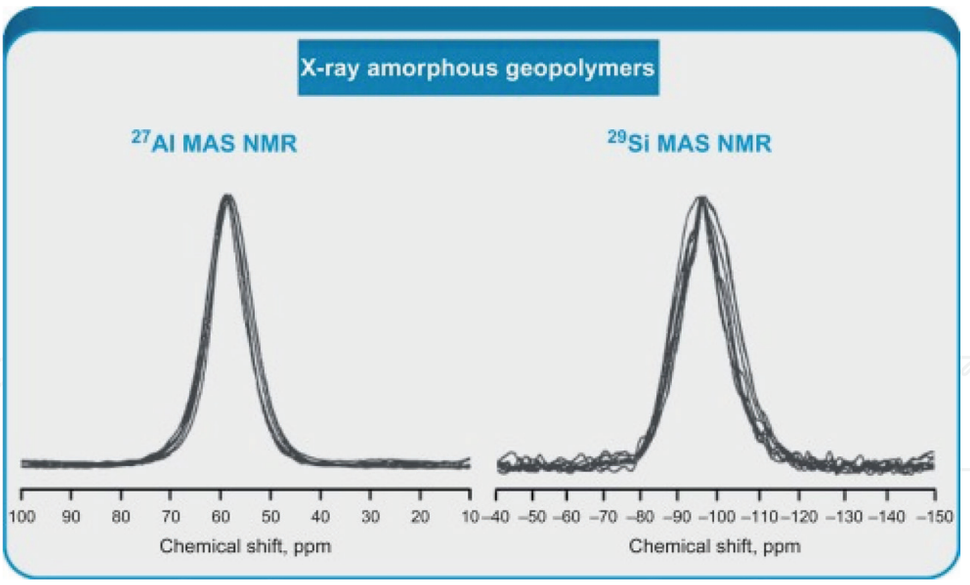

Figure 13.
The shift in wavelengths in the case of aluminum and silicon in aluminosilicate geopolymers. The first peak is for aluminum-based and the second peak is for silicon-based amorphous polymers [15].

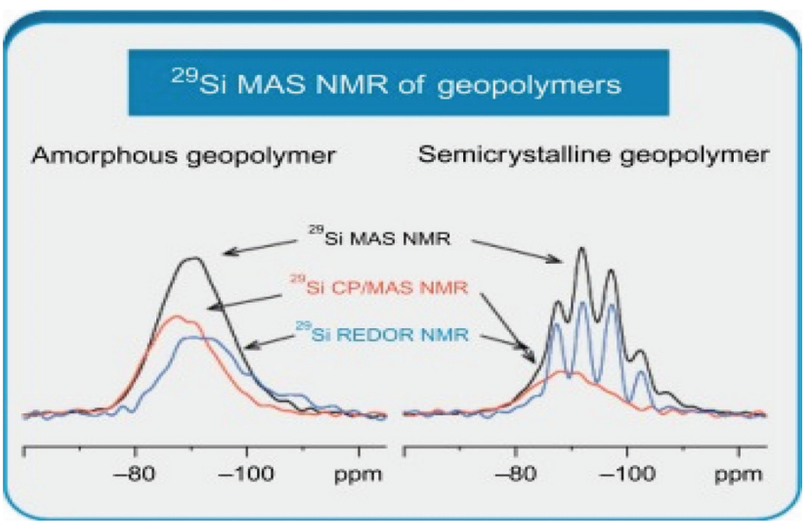

Figure 14.
Shift in amorphous geopolymer as compared to semi-crystalline geopolymers [15].

where T can be either Al or Si [15]. Fly ash and consolidated materials have been studied using NMR. The signals obtained are wide in nature, indicating a heterogeneous distribution of Si atoms in these matrices [16].

According to the 29Si RMN MAS spectra of fly ash-based geopolymer, the main shift equal to −94,66 ppm indicates the presence of Q4 (2 Al) and Q4 (3Al) units in the geopolymer matrix [17]. The shift equal to −107 ppm corresponding to the Q4 (0Al) coordination was less represented, which points to the Al penetration into the [SiO4] 4- skeleton. This interpretation of the NMR spectra is also shared by other workers [18, 19].

5. FTIR spectra

A schematic diagram of FTIR spectroscopy is reported in **Figure 15**. There is a broadband infrared source, which gives radiation. This radiation is split in the beam splitter. The split beam gets deflected onto the sample through a parabolic mirror.

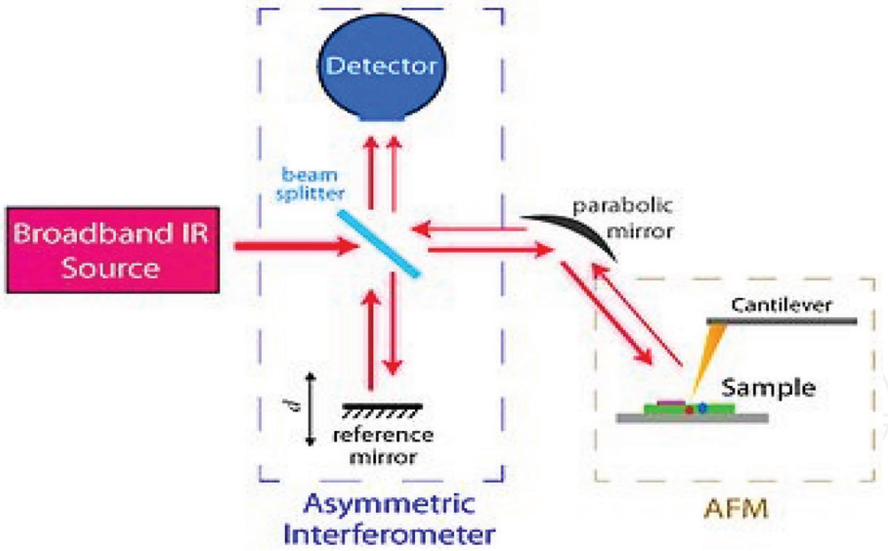

Figure 15.
Schematic of FTIR spectroscope.

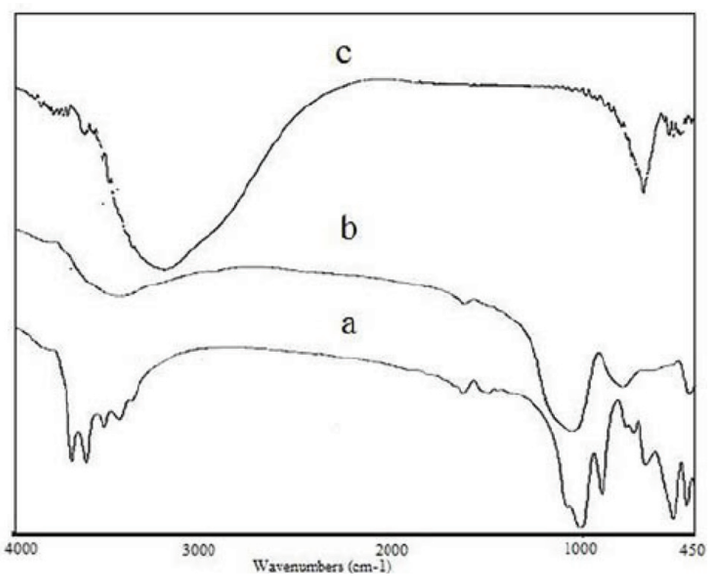

Figure 16.
Spectra for (a) soft kaolin and (b) metakaolin [15].

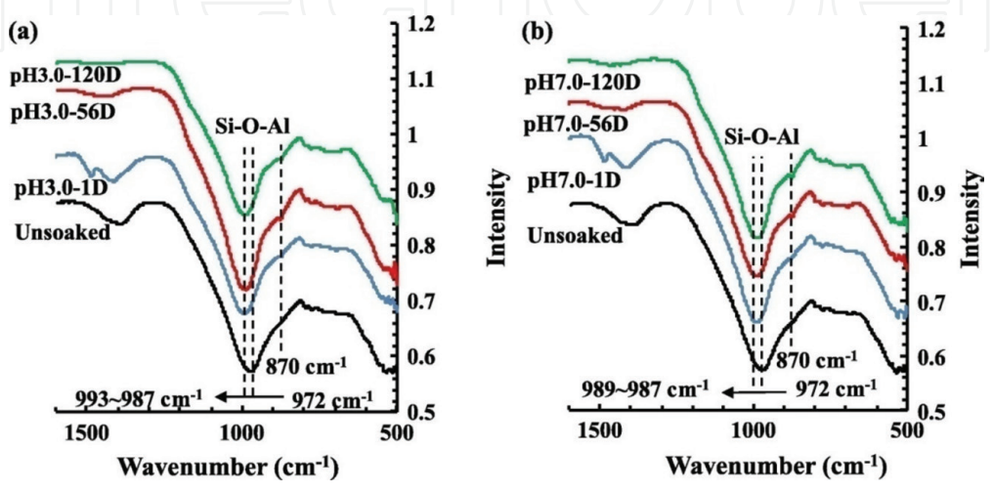

Figure 17.
FTIR spectra of unsoaked RFFG sample and RFFG samples soaked in (a) sulfuric acid (pH = 3.0) and (b) deionized water (pH = 7.0) for 1, 56 and 120 days [20].

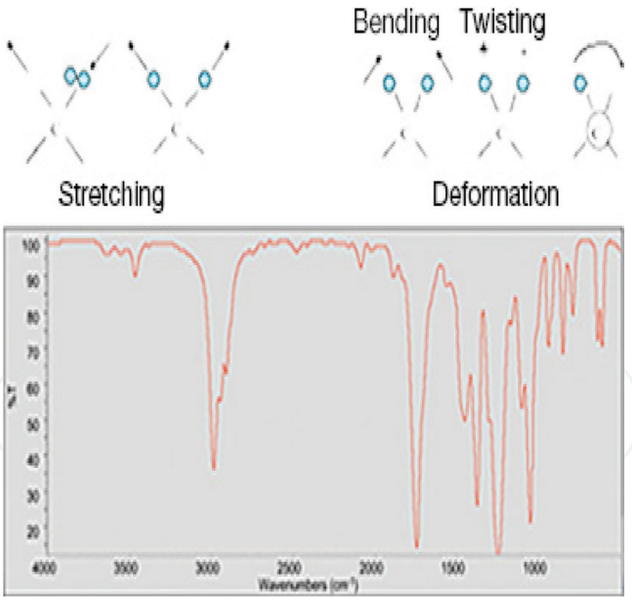

Figure 18.
Stretching, bending and twisting as seen in FTIR spectra.

The sample is kept in an atomic force microscope. The radiation from the reflection from the sample is detected using a detector.

Figure 16 gives the difference between the spectra for soft kaolin and metakaolin. There is a distinct change in the spectral lines. Comparison of spectra for red mud fly ash-based geopolymers is given in **Figure 15**.

The vertical dotted lines in **Figure 17** both indicate the position of the asymmetric stretching vibration band of Si-O-T for geopolymer gels. The dip or movement of the Si-O-T bond has to be carefully noticed while interpreting results.

Generally, as shown in **Figure 18**, stretching, bending and twisting are clearly seen as dips in the FTIR.

6. Synchrotron

A synchrotron is a high energy device in which particles are accelerated to a very high voltage. **Figure 19** is a schematic diagram of a synchrotron.

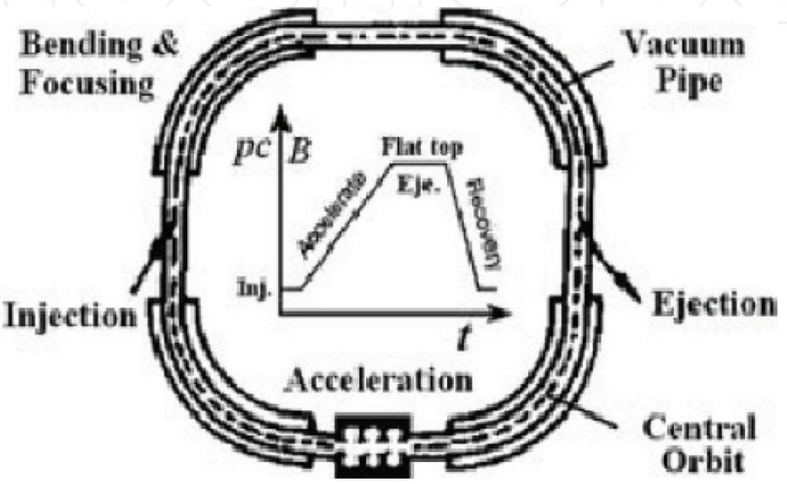

Figure 19.
A schematic of a synchrotron.

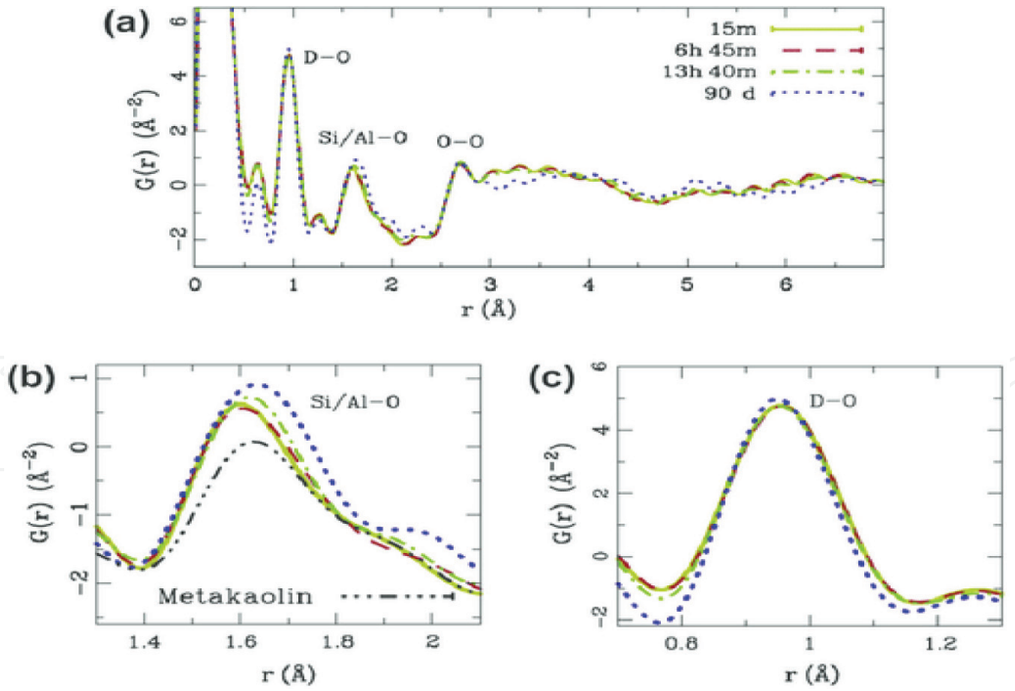

Figure 20.
Synchrotron infrared microscopy of metakaolin-based geopolymer [21].

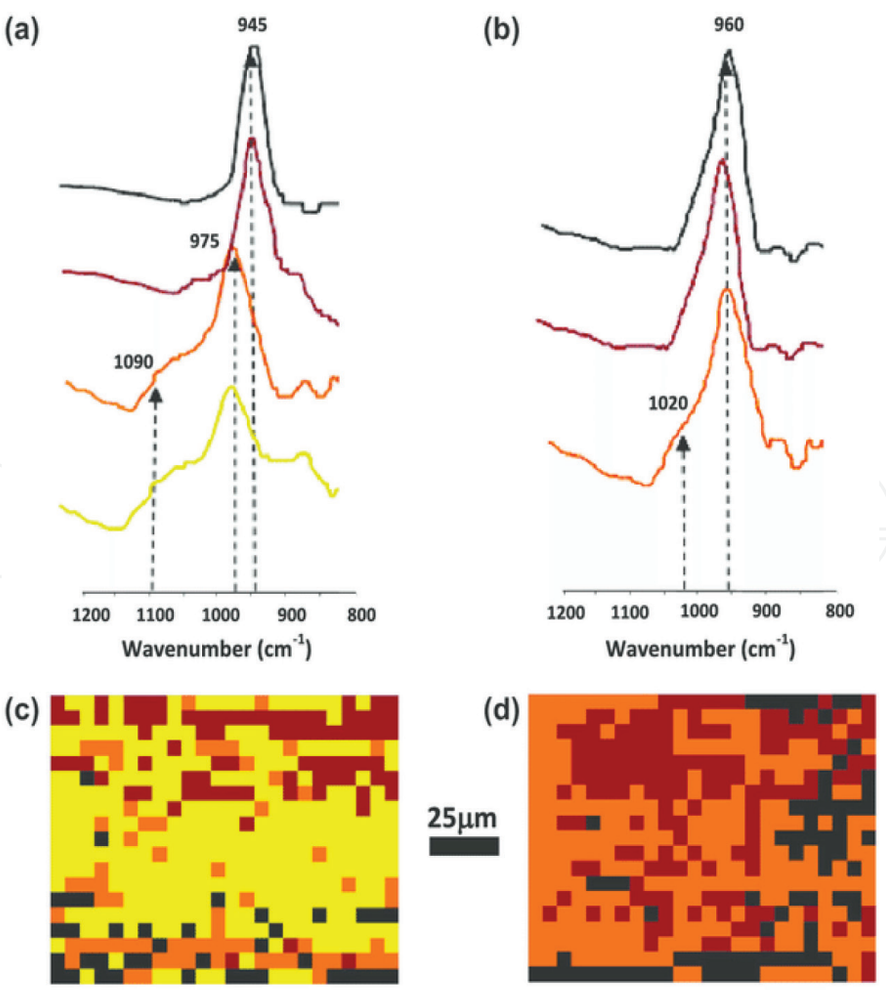

Figure 21.
Synchrotron peaks (a) without and (b) with seeding [21] already given as [21].

A **synchrotron** is a special type of cyclic particle accelerator. It is a modified form of cyclotron, in which the accelerating particle beam travels around a fixed closed-loop path. The magnetic field bends the particle beam into a closed path. This magnetic field increases with time during the accelerating process. The increased magnetic field is *synchronized* to the increasing kinetic energy of the particles. The concept of synchrotron facilitated and enabled the building of large scale research facilities to study particles in greater detail. Bending, beam focusing and acceleration can be separated into different components. The most powerful modern particle accelerators use versions of the basic synchrotron design. The largest synchrotron-type accelerator, also the largest particle accelerator in the world, is the 27-kilometer-circumference (17 mi) Large Hadron Collider (LHC) near Geneva, Switzerland, built in 2008 by the European Organization for Nuclear Research (CERN). It can accelerate beams of protons to an energy of 6.5 teraelectronvolts (TeV).

The block diagram shown in **Figure 19** shows the particles subjected to acceleration, injection, bending and focusing and final ejection.

Figure 20 reports a typical synchrotron infrared spectrum of a metakaolin-based geopolymer. Information on the Si/Al-O bonds can be deduced from this spectrum. Homogeneity of distribution can be determined using this data. This is an important result with consequences in geopolymer mix design for optimal gel structure and stability.

Synchrotron infrared microscopy data for geothermal silica-sodium aluminate geopolymer binders have been generated by John L. Provis et al. **Figure 21** shown above gives the synchrotron peaks without (a) and with 0.5 wt.% nano-Al_2O_3 seeding (b).

7. Conclusions

A summary of selected characterization techniques that have been used to study geopolymers has been given in this chapter. Some concrete examples of research work on geopolymers have been reviewed, and characterization techniques that have been practically applied in research have been explained.

Acknowledgements

I thank Intech Publishers for motivating me to write this chapter. I thank the management, SSN College of Engineering, for the academic freedom given. I thank all members of my family for their encouragement and help offered at various times.

Author details

Dattaguru Ananthapadmanaban
Department of Mechanical Engineering, SSN College of Engineering, Chennai, India

*Address all correspondence to: ananthapadmanaban.dattaguru@gmail.com

References

[1] van Deventer JSJ, Provis JL, Duxson P. Technical and commercial progress in the adoption of geopolymer cement. Minerals Engineering. 2012;**29**:89-104

[2] Shi C, Krivenko PV, Roy DM. Alkali-Activated Cements and Concretes. Abingdon (UK): Taylor & Francis; 2006

[3] van Deventer JSJ, Provis JL, Duxson P, Brice DG. Chemical research and climate change as drivers in the commercial adoption of alkali activated materials. Waste and Biomass Valorization. 2010;**1**:145-155

[4] Nikolov A, Rostovsky I, Nugteren H. Geopolymer materials based on natural zeolite. Case Studies in Construction Materials. 2017;**6**:198-205

[5] Zhuang XY, Chen L, Komarneni S, Zhou CH, Tong DS, Yang HM, et al. Fly ash-based geopolymer: Clean production, properties and applications. Journal of Cleaner Production. 2016;**125**:253-267

[6] Louati S, Baklouti S, Samet B. Geopolymers based on phosphoric acid and illito-kaolinitic clay. Advances in Materials Science and Engineering. 2016;**2016**:2359759

[7] Eberle AL, Mikula S, Schalek R. High-resolution, high-throughput imaging with a multibeam scanning electron microscope. Journal of Microscopy. 2015;**259**(2):114-120

[8] Medri V, Fabbri S, Dedecek J, Sobalik Z, Tvaruzkova Z, Vaccari A. Role of the morphology and the dehydroxylation of metakaolins on geopolymerization. Applied Clay Science. 2010;**50**:538-545

[9] Temujin J, Jadambaa T, Burmaa G, Erdenechimeg S, Amarsanaa J, MacKenzie KJD. Ceramics International. 2004;**30**:251-255

[10] Sharma AK, Sivapullaiah PV. Ground granulated blast furnace slag amended fly ash as an expansive soil stabilizer. Soils and Foundations. 2016;**56**(2):205-212

[11] Muhammad Faheem MT, Mustafa Al Bakri AM, Kamarudin H, Binhussain M, Ruzaidi CM, Izzat AM. Application of clay-based geopolymer in brick production: A review. Advanced Materials Research. 2013;**626**:878-882

[12] Cui X-M, Zheng G-J, Han Y-C, Feng S, Ji Z. A study on electrical conductivity of chemosynthetic Al_2O_3-$2SiO_2$ geopolymer materials. Journal of Power Sources. 2008;**184**:652-656

[13] Lee S, Jou H-T, van Riessen A, Rickard WDA, Chon C-M, Kang N-H. Three-dimensional quantification of pore structure in coal ash-based geopolymer using conventional electron tomography. Construction and Building Materials. 2014;**52**:221-226

[14] Das S, Yang P, Singh SS, Mertens JCE, Xiao X, Chawla N, et al. Effective properties of a fly ash geopolymer: Synergistic application of X-ray synchrotron tomography, nanoindentation, and homogenization models. Cement and Concrete Research. 2015;**78**(Part B):252-262

[15] Duxson P, Provis JL, Lukey GC, Separovic F, van Deventer JSJ. ^{29}Si NMR study of structural ordering in aluminosilicate geopolymer gels. Langmuir. 2005;**21**(7):3028-3036

[16] Alehyen S, EL Achouri M, Taibi M. Characterization, microstructure and properties of fly ash-based geopolymer. Journal of Materials and Environmental Science. 2017;**8**(5):1783-1796

[17] Bansal NP, Singh JP, Kriven WM, Schneider H. Ceramic Transactions. 2003;**153**:175

[18] Singh PS, Bastow T, Trigg M. Journal of Materials Science. 2005;**40**:3951

[19] Hoa JP, Mccormick PG, Byrne LT. Journal of Materials Science. 2002;**37**:2311

[20] Zhang M, Zhao M, Zhang G, Mann D, Lumsden K, Tao M. Durability of red mud-fly ash based geopolymer and leaching behavior of heavy metals in sulfuric acid solutions and deionized water. Construction and Building Materials. 2016;**124**:373-382

[21] Provis JL, Hajimohammadi A, White CE, Bernal SA, Myers RJ, Winarski RP, et al. Nanostructural characterization of geopolymers by advanced beamline techniques. Cement and Concrete Composites. 2013;**36**:56-64